PHYSICAL REVIEW B VOLUME 40, NUMBER 12 15 OCTOBER 1989-II

Spectroscopic investigation of the electronic states in narrow coupled GaAs/AlAs quantum wells with indirect band structure

R. Cingolani, L. Tapfer, Y. H. Zhang, R. Muralidharan, and K. Ploog
Max-Planck-Institut für Festkörperforschung, Postfach 80 06 65, D-7000 Stuttgart 80, Federal Republic of Germany

C. Tejedor
Departemento de Física Materia Condensada, Universidad Autonoma de Madrid, E-28049 Madrid 34, Spain
(Received 20 April 1989)

The optical properties of a specially designed GaAs/AlAs superlattice consisting of a periodic sequence of coupled quantum wells (CQW's) have been investigated by low- and high-excitation-intensity photoluminescence and photoluminescence excitation spectroscopy. The artificially layered semiconductor structure was grown by molecular-beam epitaxy and its structural parameters have been determined by x-ray diffraction. It exhibits the unique feature of symmetrically coupled quantum wells via the Γ states and asymmetrically coupled quantum wells via the X states. The observed luminescence shows mainly type-II emission and a weak direct recombination characterized by a splitting of the emission band due to the symmetric-antisymmetric states in the coupled wells. At high photogenerated carrier density, the type-I recombination becomes dominant. The fine structure of the observed spectral features have been interpreted on the basis of a simple quantum-mechanical calculation for the band structure of the coupled-quantum-wells system, assuming two independent sets of coupled wells associated with the AlAs X-point and GaAs Γ-point states, and also by means of a tight-binding model.

I. INTRODUCTION

The electronic properties of coupled-quantum-well (CQW) systems have recently attracted great attention.[1-5] The confined states in the quantum wells of these artificially layered semiconductor structures are strongly coupled through narrow barriers. This coupling results in a splitting of the electron and hole states corresponding to the symmetric and antisymmetric linear combinations of the electron (hole) wave functions. In addition, recent dramatic progress in the epitaxial growth techniques allows one to fabricate exactly tailored asymmetric heterostructures, thus intentionally changing the superlattice symmetry group. This results in interesting nonlinear optical properties which have recently been investigated theoretically.[6] The study of the optical transitions in these CQW heterostructures can provide detailed information on the impact of the coupling of the electron and/or hole states on the band-structure properties.

In this paper we present the results of an extensive spectroscopic investigation of the electronic properties of a GaAs/AlAs superlattice consisting of several coupled quantum wells produced by ultrathin well and barrier layers. The superlattice parameters have been determined by means of x-ray diffraction experiments. Photoluminescence, photoluminescence excitation, and high-excitation intensity luminescence spectroscopy have been carried out in order to study the optical transitions involving different subbands in the superlattice. The experimental results have been compared with a simple quantum-mechanical model calculation for the subband energies.

II. EXPERIMENT

The investigated superlattice consists of 30 coupled GaAs quantum wells having 2.2 nm width, separated by an AlAs spike of 1.2 nm thickness and sandwiched between 3.7-nm AlAs barriers (see the inset of Fig. 1). The sample was grown by molecular-beam epitaxy (MBE) on a semi-insulating GaAs substrate using a growth rate of 1 monolayer per 4 s and a growth interruption of 5 s at each of the constituent interfaces. The superlattice structure properties were investigated by means of single- and double-crystal x-ray diffraction using Cu $K\alpha_1$ radiation.

Continuous-wave (cw) luminescence and luminescence excitation measurements were carried out in the temperature range 300 K by using a Kr^+ laser and/or a conventional light source dispersed by a double monochromator. The luminescence was dispersed and analyzed by a 1-m single monochromator equipped with a cooled photomultiplier in the photon-counting mode. A high-power pulsed dye laser was used for nanosecond high-intensity excitation with a similar experimental setup and a boxcar integrator.

III. RESULTS AND DISCUSSION

A. Structural investigation

The structural properties of the superlattice consisting of a periodic sequence of CQW's are studied by using a single-crystal as well as a double-crystal x-ray diffractometer. The double-crystal method is used to record a high-resolution diffraction pattern around the

(400) reflection with Cu $K\alpha_1$ radiation in order to determine the average Al mole fraction x in one superlattice unit cell ($x=0.53$). The superlattice structure is then further investigated by recording the diffraction pattern in the vicinity of the quasiforbidden (200) GaAs reflection with the single-crystal diffractometer. The quasiforbidden (200) reflection is very sensitive to the Al modulation in the direction of the layer sequence[7] and thus to the configuration of one superlattice period. This reflection geometry is therefore appropriate to study the CQW structure.

In Fig. 1 we show the single-crystal x-ray diffraction pattern around the (200) GaAs reflection. The satellite peaks up to the third order are well observable. The angular distance between the satellite peaks is related to the superlattice period length Λ_{SL} by the equation

$$\Delta\theta=\lambda(2\cos\theta_B\,\Lambda_{SL})^{-1}\,, \tag{1}$$

where λ is the x-ray wavelength ($\lambda_{\mathrm{Cu}\,K\alpha_1}=1.540\,562$ Å) and θ_B is the kinematical Bragg diffraction angle. The superlattice period length is found to be $\Lambda_{SL}=94$ Å. Since the average mole fraction x of the superlattice unit cell is related to the ratio between the total AlAs and GaAs layer thicknesses t_{AlAs} and t_{GaAs} by $x=t_{\mathrm{AlAs}}/(t_{\mathrm{AlAs}}+t_{\mathrm{GaAs}})$, we can conclude that for our sample the total thickness of the AlAs layers is nearly equal to the total thickness of the GaAs layers.

In the case of a conventional superlattice consisting of a periodic sequence of one AlAs region and one GaAs region of approximately equal thicknesses, it is well known that the even-order satellite peaks around the (200) reflection are very weak or vanishingly small. On the contrary, in our diffraction pattern shown in Fig. 1 the second-order satellite peaks (±2) are very strong and exhibit an intensity comparable to the first-order peaks (±1). This finding indicates the existence of an additional periodicity with almost half the period length of the superlattice period in the investigated sample. An accurate interpretation of the measured diffraction pattern is performed by calculating the structure factor F_L of one superlattice unit cell for the ($L00$) reflection.[8] This F_L factor can be expressed in an analytical form for a superlattice unit cell composed of M layers as

$$F_L=2\sum_{i=1}^{M}\left[(f_{\mathrm{As}}+f_{\mathrm{AlGa}}\mathrm{R}_i^{1/2})\frac{\mathrm{R}_i^{n_i}-1}{\mathrm{R}_i-1}\prod_{k=0}^{i-1}\mathrm{R}_k^{n_k}\right] \tag{2}$$

with $n_0=0$, $\mathrm{R}_0=1$ and $\mathrm{R}_i=\exp(2\pi iLd_i/\Lambda_{SL})$, and where f_{As} and f_{AlGa} are the atomic scattering factors of As and Al or Ga atoms, respectively. The exponent n_i indicates the number of monolayers constituting the ith layer and d_i is the monolayer distance. Using this model we obtain for the GaAs constituent layers an $L_z=22$ Å and for the AlAs barrier and the AlAs spike a thickness of $L_b=37.6$ Å and $L_{sp}=12.5$ Å, respectively. These values are in good agreement with the chosen growth parameters. In Fig. 2 we show the calculated (200) x-ray diffraction patterns (a) with and (b) without the AlAs spike. The second-order satellite peaks are not observed for the case where the AlAs spike is absent, but they are well pronounced and strong in intensity for the case with the AlAs spike in the GaAs well. The calculated diffraction

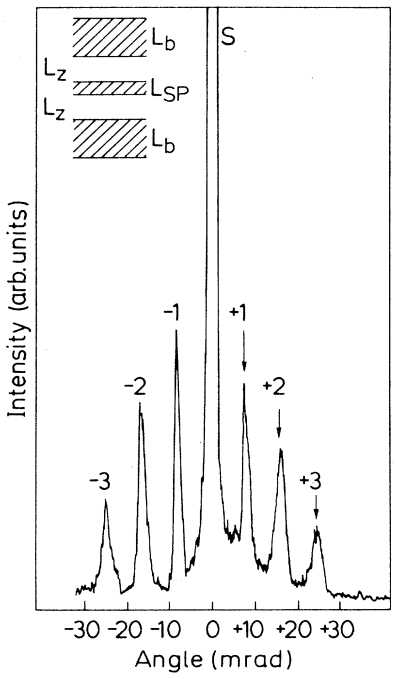

FIG. 1. Single crystal x-ray diffraction pattern in the vicinity of the quasiforbidden (200) GaAs reflection (Cu $K\alpha_1$ radiation) of the CQW heterostructure. In the inset a unit cell of the superlattice is depicted (the AlAs layers are represented by shaded regions).

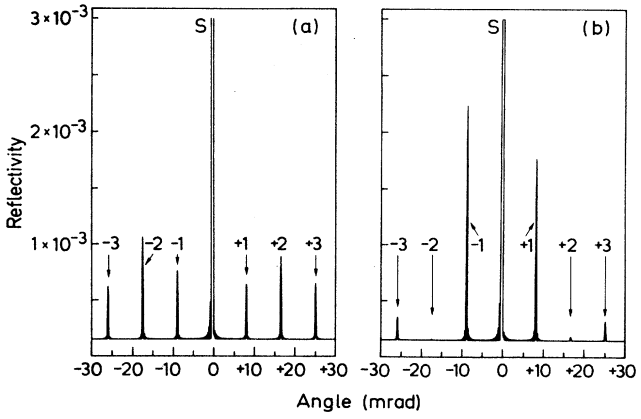

FIG. 2. Calculated (200) diffraction pattern (a) with and (b) without AlAs spike in the GaAs well. S indicates the substrate and the zeroth-order superlattice peak. The intensity of the second-order satellite peaks are related to the thickness of the AlAs spike.

pattern in Fig. 2(a) is in very good agreement with the experimental data (Fig. 1). However, the second- and third-order satellite peaks are reduced in intensity as compared to the first-order satellite, since they are more strongly affected by thickness fluctuations and interface roughness.[7] From the half-width at half maximum of the satellite peaks we additionally estimate that the constituent layer thickness fluctuates by about 1 monolayer (interface roughness).

B. Theoretical calculations of the subband energies

We have used two different theoretical models to analyze our results: an approximated square-well model with effective masses and a tight-binding calculation. The real-space energy-band diagram of the investigated CQW structure is schematically shown in Fig. 3. The superlattice consists of a periodic sequence of two thin GaAs wells (having equal thicknesses of approximately 8 monolayers) sandwiched between two AlAs barriers (13 monolayers thick). The two quantum wells are spatially separated by a narrow AlAs spike about 4 monolayers thick. Electrons (holes) with Γ-point symmetry properties experience the confining potential of the AlAs barriers which confine them in the GaAs layer [e (h) subbands in Fig. 3]. Moreover, due to the narrow AlAs spike, the well subbands are strongly coupled and thus split into symmetrical (e or h) and antisymmetrical (e^a or h^a) states. The described heterostructure should thus behave essentially like a symmetrically coupled quantum well with direct-band-gap properties. However, the narrowness of the constituent layers and the valence-band offset cause the confined electron states in the GaAs well to be at higher energy than the X-point states in the AlAs barrier, which then become the lowest electron energy levels of the system. Hence, electrons at the AlAs X point will experience the potential barrier of the higher-energy GaAs X states (due to the valence-band offset), thus being confined in the AlAs layers (e^x subbands in Fig. 3). It is therefore expected that the superlattice of Fig. 3 behaves like a type-II superlattice with a staggered band alignment. In addition, owing to the different constituent barrier thicknesses L_b and L_{sp}, the confined X-point states will have different energies in the AlAs spike (e^x_{sp} subband in Fig. 2) and in the thicker AlAs barrier (e^x_i subbands).

The above-discussed band-structure properties are qualitatively summarized in the real-space energy-band diagram of Fig. 3. The superlattice thus consists of a periodic sequence of direct symmetric CQW's (Γ well, solid line) and of a periodic sequence of indirect asymmetric CQW's (X well, dashed line). The main impacts of this complex band structure are the generation of the energy splitting of the Γ-point subbands and the rise of two different sets of X-point confined levels belonging to the different AlAs barriers.

First, we have calculated the quantized subbands for the discussed superlattice configuration by using a simple quantum-mechanical approach, i.e., by solving the Schrödinger equation of a particle in the Γ potential of Fig. 3 and adopting the envelope-function approximation with the effective-mass parameters for GaAs and AlAs in the Γ point. The eigenstate energies then result by the numerical solution of the following equations:

$$[1-\alpha^2\coth(K_bL_{sp}/2)]\tan(K_wL_z)+\alpha[1+\coth(K_bL_{sp})]=0 \quad (3)$$

for the symmetric states and

$$[1-\alpha^2\tanh(K_bL_{sp}/2)]\tan(K_wL_z)+\alpha[1+\tanh(K_bL_{sp})]=0 \quad (4)$$

for the asymmetric states. In Eqs. (4) and (5) $K_w=(2m_w/h^2E)^{1/2}$, $K_b=[2m_b/h^2(V-E)]^{1/2}$, and $\alpha=K_wm_b/K_bm_w$, where m_w and m_b are the effective masses in the well and in the barrier, respectively. The

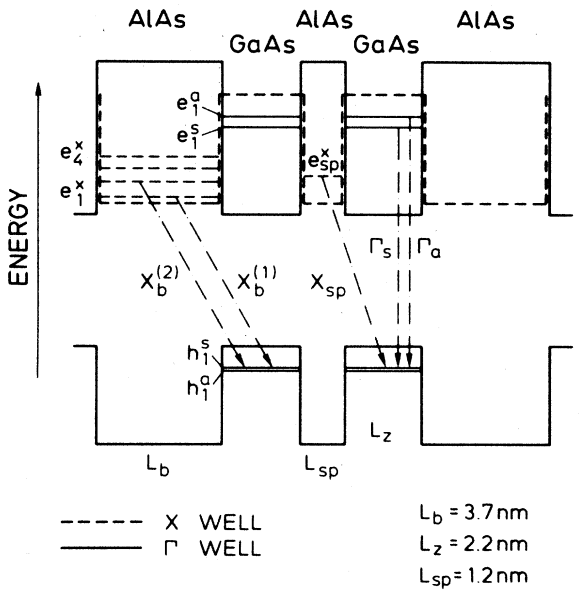

FIG. 3. Scheme of the real-space energy band structure of the investigated superlattice. The solid lines represent the symmetric coupled wells originating from the band discontinuities at the GaAs and AlAs Γ points (Γ wells). The dashed lines indicate the asymmetric indirect coupled wells originating from the band discontinuities at the semiconductor X points (X wells). The subbands labeled e_i^x belong to the X wells (the subindex sp stands for AlAs spike subband). The order of the confined states is indicated by the numerical index $i=1,2,\ldots,n$. The Γ-well electron subbands are labeled $e_i^{a,s}$ (or $h_i^{a,s}$ for the hole subbands), where the index a or s means antisymmetrical or symmetrical energy levels in the CQW. The main optical transitions discussed in the text (dashed-dotted lines) are labeled $X_b^{(i)}$ and $X_{sp}^{(i)}$ for the X-wells emission from the AlAs barrier and AlAs spike, respectively, while they are labeled Γ_a and Γ_s for the direct CQW emissions involving antisymmetric or symmetric states, respectively. L_b, L_{sp}, and L_z indicate the width of the AlAs barrier and spike layers and of the GaAs well layer, respectively.

symmetrical and antisymmetrical solution of Eqs. (3) and (4) give a splitting for the electron Γ states of the order of 25 meV and of about 2 meV for the heavy-hole subbands.

The *X*-electron states confined in the AlAs spikes and in the AlAs barrier have been assessed by means of a Kronig-Penney calculation treating the periodic sequences of the different AlAs layers like independent superlattices. In Table I we summarize the results of the described simple calculations for the assessment of the fundamental optical transitions among the quantized states depicted in Fig. 3.

In order to examine the existence of coupling effects between the *X*-well electron states through the GaAs layers, we apply the theoretical model developed by Yariv *et al.*[9] This model represents in analytical approach based on the linear combination of well orbitals to solve the Schrödinger equation in the investigated CQW system. The main results of this model are the introduction of two parameters, namely k and d, which respectively account for the electronic level splitting and for the electronic localization. In particular, the wave function of an electron in the potential of Fig. 3 can be expressed as a linear combination of the electronic wave functions of the constituting uncoupled quantum wells. In the limit of weak coupling, this assumption leads to a determinantal equation whose solutions are of the type

$$\varepsilon=\pm(d^2+k_1k_2)^{1/2}\,, \tag{5}$$

where $d=(E_1-E_2)/2$ and $k_{1,2}=2[(E_1+E_2)/Kt_{1,2}]\times\exp(-KL)$. In Eq. (5) E_1 and E_2 are the subband energies of the uncoupled quantum wells, $K=\{2m/h^2[V-(E_1+E_2)/2]\}^{1/2}$, where V is the potential barrier through which the wells are coupled, t_1 and t_2 are the widths of the coupled quantum wells, and L is the coupling barrier width. The subband energies are then given by

$$e_i(\pm)=\tfrac{1}{2}(E_1+E_2)\pm\varepsilon\,, \tag{6}$$

corresponding to the eigenenergies of the symmetrical and antisymmetrical solutions of the Schrödinger equation in the CQW. It is therefore evident that the energy splitting due to the well coupling is given by 2ε.

In the case of the asymmetrically coupled *X* wells the electron subbands have considerably different energies, owing to the different thicknesses of the AlAs barrier and AlAs spike, and they experience a potential barrier of about 0.38 eV. From Eq. (5) the weak coupling of the *X* wells through the GaAs layer [$\exp(KL)=10^{-3}$] then results in a negligible value of the k_1k_2 product, thus giving $\varepsilon\cong 2d$. From Eq. (6) it is easily found that the symmetric and antisymmetric states become $E_a=(E_1+E_2)/2+d$ and $E_s=(E_1+E_2)/2-d$, i.e., they are almost coincident with the energy levels of the uncoupled *X* wells. Therefore, in spite of the narrowness of the GaAs layers, which actually acts like a barrier for the electrons confined at the AlAs *X* point, no splitting is expected for the quantized subbands in the *X* wells.

In order to get more insight in the band structure of our system, we have performed a second calculation by using a tight-binding scheme. A detailed explanation of the method and its application to different material systems is given by Brey and Tejedor in Ref. 10. The model is based on a simple perturbative approach for the solution of the tight-binding Hamiltonians and includes the coupling between Γ and *X* states. A discussion of the comparison between theoretical calculations and experimental data given in Table I will be made in the following.

In the calculations only optical transitions involving heavy-hole subbands have been considered, since most of the experimental data to be compared have been measured at low temperature, when no population of the light-hole states is expected.

TABLE I. Comparison between the experimental and calculated energies of the optical transitions in the investigated superlattice. The values are expressed in eV (nm). The optical transitions are labeled according to the notation of Fig. 2.

Transition	Square well	Experimental	Tight binding
$X_b^{(1)}$	1.713 (723.6)	1.730 (716.5)	1.741 (712.0)
X_{sp}	1.782 (695.6)	1.781 (696.0)	1.800 (688.7)
Γ_s	1.84 (672.2)	1.836 (675.2)	1.904 (651.1)
Γ_a	1.871 (662.5)	1.854 (668.6)	1.963 (631.5)

C. Spectroscopic investigations

On the basis of the described theoretical considerations we next give a tentative interpretation of the observed luminescence features. In Fig. 4 we show the low-temperature photoluminescence (PL) and photoluminescence excitation (PLE) spectra. The latter is detected at the emission wavelength of the expected type-II radiative recombination. The spectra clearly show an energy shift

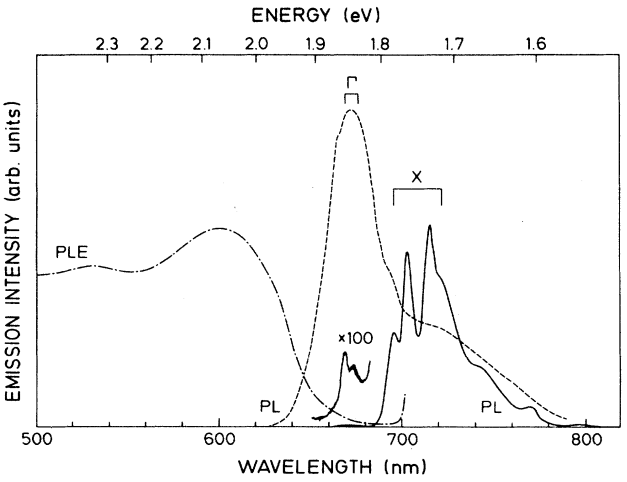

FIG. 4. Comparison between the photoluminescence excitation (PLE) and photoluminescence spectra (PL lines) recorded at 4 K. The solid-line PL spectrum is measured under low-power cw excitation, whilst the broken-line PL spectrum is measured under nanosecond pulsed excitation. The Γ doublet is amplified 100 times to be compared with the pulsed spectrum.

between the direct absorption edge and the space-indirect luminescence occurring around 1.73 eV. In the cw luminescence spectrum a weak emission peak in the high-energy region is observed. This feature is located around 1.84 eV and shows a doublet structure with a splitting of about 20 meV.

The observed PLE spectrum is characteristic for type-II GaAs/AlAs superlattices with staggered band alignment. As widely demonstrated in the literature (see, for example, Ref. 11), the PLE spectrum of a type-II superlattice exhibits a weak structure around the energy of the type-II emission, owing to the small absorption coefficient of the space-indirect transition, and a sharp onset at higher energy, due to the large direct absorption coefficient. This finding allows us to attribute the observed luminescence to space-indirect radiative transitions involving X-point electrons confined in the AlAs slabs and Γ-point holes confined in the GaAs wells. However, it should be noted that the measured PLE spectrum does not show a sharp direct absorption onset but a smooth increase in the energy region between the X and Γ states. This feature can be ascribed to two different phenomena. First, the effect of the layer-thickness fluctuations in the investigated multi-interface structure gives rise to localized states where carriers can be trapped, thus giving an enhancement of the absorption out of the expected resonant levels. Second, two sets of states belonging to the two different X wells are expected to fall in the energy range between the lowest quantized X band and the lowest quantized Γ band (e^x_{sp} and e^x_i states in Fig. 3), leading to an increase of the density of states below the direct onset. Nevertheless, the comparison of the luminescence and PLE spectra in Fig. 4, allows us to ascribe the weak doublet structure around 1.84 eV to the type-I emission (from Γ-point states), which also confirms the predicted energy splitting due to the well coupling. A more detailed interpretation of the type-II luminescence fine structure is more complex and will be attempted in the following.

In Fig. 5 we show several low-temperature emission spectra recorded at different excitation intensities ($I_0=2$ W/cm^2). The observed luminescence is shifted by about 100 meV with respect to the direct emission, and is then clearly related to type-II transitions involving electrons confined in the X wells. The main feature of the observed spectra is the existence of several sharp lines distributed in the spectral range between 700 and 800 nm. At the lowest excitation intensities the X'_{sp} line is dominant while several structures arise on its low-energy side. When we increase the excitation intensity, the doublet structure labeled X_{sp} and X'_{sp} tends to saturate whilst the X_b and X'_b lines become dominant. In addition, a few equally spaced shoulders can be observed on the low-energy side of the emission curve.

The attribution of these lines can tentatively be carried out on the basis of the calculated transition energies given in Table I. We first note that the energy separation between the X_b and the X_{sp} lines roughly corresponds to the calculated energy difference between the electronic subbands confined in the AlAs barrier and the AlAs spike (the e^x_1 and e^x_p subbands shown in Fig. 3). This finding indicates that these two lines arise from the space-indirect radiative recombination of X-point electrons confined in the AlAs slabs and Γ holes confined in the GaAs well. Particularly, according to the different well width in the X-point CQW system, the high-energy X_{sp} line can be attributed to the type-II transition originating in the AlAs spike, while the X_b line is ascribed to the type-II transitions from the larger AlAs barrier. The calculated transition energies support this attribution (see Table I). Both the tight-binding and the square-well model predict a splitting between 60 and 70 meV between the $X_b^{(1)}$ and the X_{sp}, to be compared with the experimental value of 51 meV. In particular, the approximated square-well model shows a satisfactory agreement with the observed luminescence energy positions if the conduction- and valence-band offset parameters are adjusted to the ratio 60:40. A larger discrepancy is found between the experimental data and the results of the tight-binding calculations made with the offset and the band-structure parameters reported in Ref. 10. Nevertheless, in the case of this

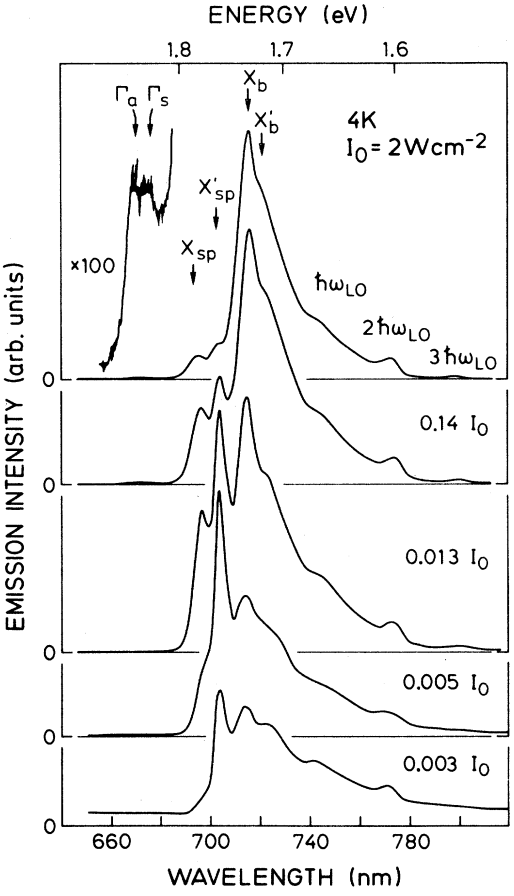

FIG. 5. Type-II X-well emission recorded at 4 K and at different excitation intensities. The spectra have been multiplied by constant factors to be compared. The transitions are labeled following the notation of Fig. 3. The Γ-well doublet structure is amplified 100 times.

more sophisticated model, the calculation of the absolute position of the optical transitions needs detailed knowledge of the effective conduction- and valence-band offset ratio. In fact, it has been recently demonstrated[12] that in heterostructures consisting of ultrathin layers, the actual band offset ratio has a critical dependence on the number of atomic monolayers constituting the slab. In the case of the investigated CQW this results in different band-gap discontinuities in the X and in the Γ wells. Since the precise evaluation of the transition energies in the ultrashort-period CQW's by means of sophisticated theoretical calculations is beyond the scope of the present work, the results of the tight-binding calculations can be used in order to test the reliability of the approximated square-well model assuming independent Γ and X wells, i.e., ultimately, the predicted energy splitting between the fundamental optical transitions and the number of transitions originating in the X and in the Γ well. It is worth noting that in the approximated square-well model an average offset ratio can be adjusted as a free parameter to better fit the experimental data, as shown in Table I. This is not possible in the tight-binding model, which is much more sensitive to the actual electronic structure of the semiconductor heterostructure. Taking into account these limitations, the comparison of the results of the two different theoretical models shown in Table I supports the interpretation of two different transitions originating in different X wells. Moreover, even with the approximation discussed above, there is a good overall agreement between the number and the energy position of the observed optical transitions and the theoretically predicted values, calculated either with the approximated or with the tight-binding model.

According to the results of the two theoretical models, no subband splitting due to the coupling through the GaAs layer is expected for the X-well states. Therefore, the remaining luminescence lines shown in Fig. 5 have to be ascribed to extrinsic recombination processes. In agreement with recent observations in ultrashort-period GaAs/AlAs superlattices,[13] the low-energy bands labeled $\hbar w_{\mathrm{LO}}$, $2\hbar w_{\mathrm{LO}}$, and $3\hbar w_{\mathrm{LO}}$ can be ascribed to phonon-assisted transitions involving AlAs LO phonons having an energy of about 50 meV. Such weak phonon replicas of the space-indirect luminescence can be considered a characteristic feature of the type-II transitions.[14] They are probably related to the fast electron transfer between points of the Brillouin zone with different k vectors, occurring in the photoexcitation processes of the Γ and X wells.

As far as the origin of the intense X'_{sp} and X'_b lines is concerned, we believe that they are related to localization phenomena due to layer fluctuations at the constituent AlAs-GaAs interfaces. In fact, even one monolayer fluctuation at the interface of the ultranarrow layers constituting the CQW structure can generate large potential fluctuations which localize the electron wave function at the AlAs-GaAs interface. Such a phenomenon can be qualitatively explained by considering the fast decay of the localization parameter k in Eq. (5) due to the exponential term, when a variation of 25% for the layer thickness L is assumed (i.e., one monolayer fluctuation for the 1.2-nm AlAs spike).[9] Under these conditions an increase of one monolayer in the AlAs spike results in a decrease of about 18 meV for the localized electron subband in the narrowest X well, in agreement with the observed energy splitting between the X_{sp} and X'_{sp} lines. Consequently, the luminescence line labeled X'_{sp} can be ascribed to such a localization phenomenon occurring in the AlAs spike X well, due to the 1 monolayer fluctuation. This attribution is confirmed by the observed temperature dependence (not shown) and excitation intensity dependence shown in Fig. 5. At the lowest excitation intensity the lower-energy localized state in the AlAs spike is populated. At a larger photogeneration rate the electron distribution function allows the population of the higher-energy fundamental e^x_{sp} state (Fig. 3), while the localized state saturates due to the smaller density of states. A similar argument can be invoked to interpret the X'_b line. In this case the effect of the potential fluctuation is smaller due to the less important percentage variation in the total thickness of the 3.7-nm AlAs barrier when 1 monolayer fluctuation is assumed. The predicted energy shift for such thickness fluctuation is of the order of 5 meV in the largest X well. Inspection of our spectra reveals that it is difficult to resolve the exact energy position of the X'_b band, which always appears as a shoulder on the low-energy side of the main X_b band. Nevertheless, this emission line shows the same temperature and intensity dependences already observed for the X'_{sp} line, thus supporting our interpretation.

The relative amplitude of the type-II transitions originating in the two different X wells should be briefly addressed. In Fig. 5 it is clearly shown that at relatively large excitation intensities the X_b transitions originating from the barrier X well become dominant, while the X_{sp} transitions from the AlAs spike saturate. We believe that this phenomenon is related to the dependence of the Γ-X electron transfer on the X-well width. In analogy to the observed increase of the carrier capture efficiency in larger direct quantum wells,[14] a similar X-well width dependence can be invoked for the transfer efficiency of photogenerated Γ-point electrons into the lower-lying X-point states. In addition, although the X_b transition is the lowest energy transition of the system, at low-excitation intensity the X_{sp} emission can be more favored by the larger overlap of the electron and hole wave functions confined in different layers owing to the thinner AlAs spike thickness. Further information on this problem could be provided by time resolved measurements of the Γ-X scattering time in these indirect CQW systems.

We finally point out the existence of a very weak emission from the direct coupled quantum wells in the spectra of Fig. 5. This emission is amplified in the maximum intensity spectrum and it exhibits the expected splitting due to the symmetric and antisymmetric linear combination of electronic states occurring in the coupled wells. It is worth noting that the luminescence efficiency of the direct Γ wells is found to be very low, about 2 orders of magnitude less than the X-well emission, at least under the adopted experimental conditions.

Dramatic changes in the radiative emission efficiency

occur under nanosecond pulsed excitation. At excitation intensities of the order of 1 MW cm^{-2} the high-density photogenerated electron-hole population relaxes in both the Γ and the X CQW's. Owing to the shorter relaxation time of the type-I transition, the direct CQW emission becomes dominant at high pumping levels while the type-II recombination shows saturation. We have previously adopted the high-intensity spectroscopy to investigate the type-I–type-II transition occurring at a certain critical thickness in symmetrical short-period GaAs/AlAs superlattices.[15] This technique allows us to study the competition between the radiative recombination channels associated with the direct Γ wells and the indirect X wells in the superlattice. The results of the measurements for the case of the investigated CQW's are shown in Fig. 6. At low excitation intensity a broad type-II luminescence appears in the spectral range of 680–800 nm, as already observed in cw measurements. When we increase the excitation intensity, band-filling effects lead to the progressive population of the higher-energy states in the indirect X wells. It is in particular possible to resolve the X_b and X_{sp} emission bands previously discussed and also the $X_b^{(2)}$ band which is probably due to the band filling of the second quantized state in the 3.7-nm AlAs well (barrier X well). At larger excitation intensity the direct Γ-well emission appears, again showing the doublet structure spaced by about 20 meV due to the subband splitting in the CQW. Under these conditions the type-II emission is completely saturated. At the maximum pumping rate the emission curve exhibits two broad bands associated with the radiative recombination of a three-component electron-hole plasma composed of Γ-point electrons, X-point electrons, and Γ-point holes. We should point out that very recently it has been theoretically predicted that in type-II superlattices a stable electron-hole liquid phase can occur.[16] In addition, a decay time in the μs scale has been measured for the type-II luminescence in GaAs/AlAs short-period superlattices.[17] According to these recent results, we cannot exclude that the high-excitation-intensity luminescence spectra of Fig. 6 can be related to the radiative recombination of electron-hole droplets or liquid associated with the space-indirect gap in the superlattice. A detailed investigation of this phenomenon is underway in this laboratory.

The observed double emission from Γ and X CQW's is finally compared in Fig. 4 with the PLE and cw PL spectra. This comparison clearly shows the presence of a dense set of states linking the lowest X-point subband and the fundamental Γ-point confined electronic state. According to the discussed spectral features and to the results of the theoretical calculations of Table I two distinct groups of optical transitions can be distinguished, which are located around 730 and 670 nm. The former is ascribed to a set of type-II transitions originating in the AlAs spike and barriers, the latter is due to the type-I recombination of electrons in the coupled symmetric and antisymmetric states at the GaAs Γ point.

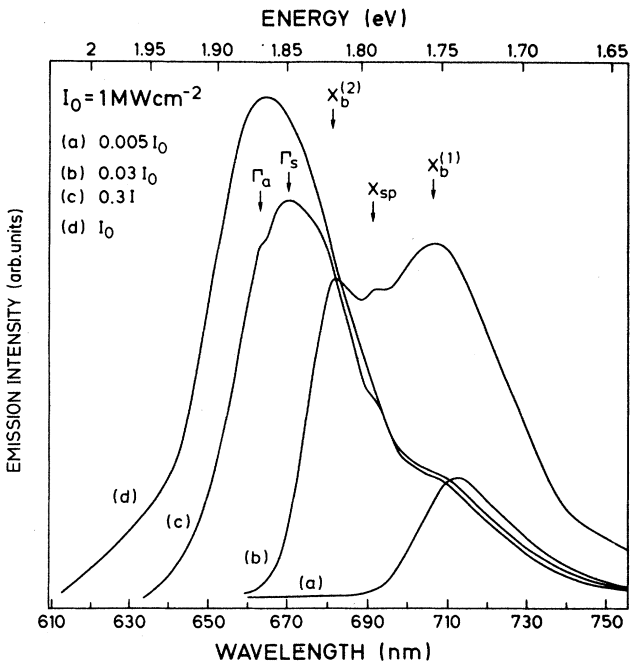

FIG. 6. High-excitation-intensity photoluminescence spectra of the CQW recorded at 4 K and at different excitation intensities. The spectra have been multiplied by constant factors to be compared.

IV. CONCLUSIONS

We have investigated the radiative recombination processes in a superlattice consisting of a periodic sequence of ultranarrow coupled GaAs/AlAs quantum wells. The actual band structure of the studied superlattice has been exemplified by assuming two separate sets of electronic subbands resulting from the confining potential at the GaAs Γ point and at the AlAs X point, respectively, coupled through the respective barriers. The energy of the type-I transitions are estimated by using a simple quantum-mechanical calculation for the coupled quantum wells separated by a thin barrier, thus predicting a symmetric-antisymmetric splitting of about 25 meV. The type-II transitions are calculated by using a Kronig-Penney potential for the wells originating from the confining potential in the AlAs slabs. The results obtained by means of these simplifying assumptions have been compared with the results of a tight-binding calculation. The structure of the investigated superlattices have been tested by means of single- and double-crystal x-ray diffraction study. The luminescence and luminescence excitation measurements show a satisfactory agreement with the predicted optical transition energies, in spite of the simplifying assumptions made in the calculations. The experimentally observed energy splitting of the type-I luminescence band well accounts for the predicted coupling effect between the direct wells. Finally, high-excitation-intensity emission spectroscopy has been performed in order to study the competition mechanisms between the type-I and the type-II radiative recombination channels, showing the impact of the band-filling effect on

the complex band structure of the investigated superlattice.

ACKNOWLEDGMENTS

The expert help of J. Nagle with the sample preparation and the arrangement to carry out part of the experimental work in the laboratories of the National Quantum Electronics Group at the Department of Physics of the University of Bari (Italy) are gratefully acknowledged. This work has been partly supported by the Bundesministerium für Forschung und Technologie (Bonn, Germany) of the Federal Republic of Germany. One of us (C.T.) acknowledges the financial support of the Comisión Asesora de Investigación Científica y Técnica (under Grant No. MAT88-0116-C02-01), Madrid, Spain.

[1]G. Bastard, U. O. Ziemelis, C. Delalande, M. Voos, A. C. Gossard, and W. Wiegmann, Solid State Commun. **49**, 671 (1984).
[2]H. Kawai, J. Kaneko, and N. Watanabe, J. Appl. Phys. **58**, 1263 (1985).
[3]Y. J. Chen, E. S. Koteles, B. S. Elman, and C. A. Armiento, Phys. Rev. B **36**, 4562 (1987).
[4]J. K. Kurghin, Phys. Rev. B **36**, 4056 (1988).
[5]S. Charbonneau, M. L. W. Thewalt, E. S. Koteles, and B. Elmann, Phys. Rev. B **38**, 6287 (1988).
[6]J. W. Little and R. P. Leavit, Phys. Rev. B **39**, 1365 (1989).
[7]L. Tapfer and K. Ploog, Phys. Rev. B **33**, 5565 (1986).
[8]J. Korvarec, M. Bandet, J. Canlet, P. Auvraj, Y. J. Emery, and A. Regreny, J. Appl. Crystallogr. **17**, 196 (1984).
[9]A. Yariv, C. Lindsey, and U. Sivan, J. Appl. Phys. **58**, 3669 (1985).
[10]L. Bray and C. Tejedor, Phys. Rev. B **38**, 9112 (1987).
[11]K. J. Moore, G. Duggan, P. Dawson, and C. T. Foxon, Phys. Rev. B **38**, 5535 (1988).
[12]N. E. Christensen, Phys. Rev. B **37**, 4528 (1988).
[13]D. S. Jiang, K. Kelting, T. Isu, H. J. Queisser, and K. Ploog, J. Appl. Phys. **63**, 845 (1988); K. J. Moore, G. Duggan, P. Dawson, C. T. Foxon, N. J. Pulsford, and R. J. Nicholas, Phys. Rev. B **39**, 1249 (1989).
[14]H. J. Polland, K. Leo, K. Rother, K. Ploog, J. Feldmann, G. Peter, E. O. Gobel, K. Fuijwara, T. Nakayama, and Y. Ohta, Phys. Rev. B **38**, 7635 (1988).
[15]R. Cingolani, M. Ferrara, L. Baldassarre, M. Lugara, and K. Ploog, Phys. Rev. B (to be published).
[16]P. Hawrylak, Phys. Rev. B **39**, 6264 (1989).
[17]P. Dawson, K. J. Moore, C. T. Foxon, G. W. 't Hooft, and R. P. M. van Hal, J. Appl. Phys. **65**, 3606 (1989).